CONF-951155--94

LA-UR 96-0287

Los Alamos National Laboratory is operated by the University of California for the United States Department of Energy under contract W-7405-ENG-36.

TITLE: Alteration History Studies in the Exploratory Studies Facility, Yucca Mountain, Nevada, USA

AUTHOR(S): Schon Levy, Steve Chipera (EES-1)
David Norman (New Mexico Tech)

SUBMITTED TO: Scientific Basis for Nuclear Waste Management XIX, Proceedings Materials Research Society Symposium V, Fall Meeting, Boston, 27 November - 1 December 1995.

Los Alamos National Laboratory
Los Alamos, New Mexico 87545

LA-UR--96-0287

ALTERATION HISTORY STUDIES IN THE EXPLORATORY STUDIES FACILITY, YUCCA MOUNTAIN, NEVADA, USA

S.S. LEVY*, D.I. NORMAN**, S.J. CHIPERA*
*Earth and Environmental Sciences Division, Mail Stop D462, Los Alamos National Laboratory, Los Alamos, NM 87545, sslevy@lanl.gov **Department of Geoscience, New Mexico Tech, Socorro, NM 87801

ABSTRACT

By mid-1995, the Exploratory Studies Facility (ESF) extended about 1.1 km from Exile Hill westward toward Yucca Mountain, mostly within densely welded, devitrified Tiva Canyon Tuff. Secondary mineral occurrences in this unit include breccia cements of mordenite, a fibrous zeolite, and vapor-phase deposits of silica, alkali feldspar, apatite, hollandite, amphibole, and zircon. Calcite is also a common secondary mineral in faults and fractures. Studies of water and gas contents in fluid inclusions in calcites from a fault in nonwelded tuff and a fracture in densely welded tuff suggest mineral deposition under transient locally saturated conditions. Calcite in the nonwelded tuff incorporated air from the unsaturated tuff adjacent to the fault.

A highly altered interval within pre-Pah Canyon tuffs just above the top of the Topopah Spring Tuff may be a fossil fumarole or other hydrothermal feature associated with cooling pyroclastic deposits, overprinted by later zeolitic alteration. The observed quartz, cristobalite, opal-CT, and fluorite have been widely identified as products of syngenetic devitrification and vapor-phase alteration in and above the Topopah Spring Tuff. Smectite, also an abundant secondary mineral at the ESF site, has been observed elsewhere at this stratigraphic level.

Zeolitic alteration of nonwelded tuffs above the Topopah Spring Tuff, as seen in the ESF, has also been noted in drill core and outcrop at northeastern Yucca Mountain. The hydrologic and geochemical conditions that favored zeolitization only in certain areas of this stratigraphic interval have yet to be determined.

INTRODUCTION

The north ramp of the Exploratory Studies Facility (ESF) is a study and access tunnel for the Yucca Mountain Site Characterization Project. By mid-1995, the ESF extended about 1.1 km from Exile Hill on a trajectory of ~299° [1] toward Yucca Mountain, a potential nuclear waste repository site in southern Nevada. Geologic features penetrated by the ESF include, heading west, the Tiva Canyon Tuff, the Bow Ridge fault with pre-Rainier Mesa tuffs downdropped west of the fault, more Tiva Canyon Tuff, and nonwelded pre-Pah Canyon tuff above the Topopah Spring Tuff (candidate host rock for the potential repository). All of these rock units are Miocene silicic pyroclastic deposits.

Alteration history research in the ESF is prioritized by impact or value for site investment analysis. Features not previously encountered, especially those indicating recent geochemical and hydrologic processes, require timely study to place them within the context of Yucca Mountain alteration. Additional goals are to describe the distribution of secondary minerals and alteration features in the ESF and to identify secondary mineral occurrences suitable for studies that increase the level of confidence in project positions on technical issues.

METHODS

ESF sample locations are measured inward from the portal. For example, a location 115 m inward is designated as Station (abbreviated Sta.) 1+15. Locations are further specified as left or right rib (wall). Vertical locations are determined with respect to the springline, a horizontal line fixed on the rib during the wall mapping activity. Project photographs YM-10396 through YM-10401 provided the basis for the stratigraphic and structural analysis of a possible fumarole.

X-ray powder diffraction data were obtained on an automated Siemens D-500 diffractometer using Cu-Kα radiation, incident- and diffracted-beam Soller slits, and a Kevex (SiLi) solid-state detector. Data were collected from 2 to 50° 2θ and count times $\geq$ 2.0 s per step. Quantitative analyses employed the internal standard method of Chung [2] using 1.0-μm corundum as the internal standard. Data-collection methods to detect erionite, with detection limits between 100 and 500 ppm, are described in [3] and [4].

Scanning-electron microscopy, utilizing an ISI model DS-130 scanning electron microscope operated at 19 kV with a Kevex model 7000 energy-dispersive X-ray analytical system, provided details of textural relations. Minerals were identified from X-ray spectra and crystal morphology.

Gas analyses of calcite fluid inclusions were conducted using a Balzers model QMG 125 quadrupole mass spectrometer. Pulses of Ar, CH_4, CO_2, He, H_2O, N_2, and O_2 from crushed samples were recorded and gas ratios were measured by integration of the mass spectra. Multiple analyses were obtained from repeated crushing of each sample. Details of sample preparation and error analyses are given in [5] and [6].

VAPOR-PHASE MINERALS AND BRECCIA CEMENTS IN THE TIVA CANYON TUFF

Abundant vapor-phase alteration products within large pumice clasts are typical of syngenetic mineral deposits near the top of the Tiva Canyon Tuff. In addition to silica, the phases are pale yellow tabular apatite, black aggregates of prismatic hollandite, orange needles of probable amphibole, flat round grains of Fe-Ti oxide, and prismatic zircons. These phases overlie older coatings of corroded potassium feldspar or spherulitic opal-CT and are themselves coated with opal. The hexagonal apatite plates are $\leq$ 300 μm across. Many smaller crystals have a skeletal morphology. The well terminated zircons are $\leq$ 20 μm long. Both minerals have potential value for geochronologic and paleothermal studies. For example, the ages of zircons in Tiva Canyon breccias are cited as evidence for or against a recent hydrothermal eruption [7]. The *in situ* origin of the ESF zircons is apparent, so that studies of these zircons could form a basis for comparison with other populations of ambiguous origin.

Breccia zones in the north ramp exposures of Tiva Canyon Tuff are common and are not typically associated with discrete faults. Crushed-tuff-matrix breccias like these usually are uncemented or contain small local deposits of secondary minerals. Quartz from Tiva Canyon breccia at Exile Hill was dated by electron spin resonance at 8.7$\pm$2.6 Myr [8]. Given the large uncertainty, the breccia is about the same age as the host tuff.

In addition to quartz, aggregates of mordenite, potassium feldspar, cristobalite, and heulandite-clinoptilolite are common weak cements in the Tiva Canyon breccias. Mordenite is a fibrous zeolite widely distributed in trace quantities. Individual crystals of the mordenite cements are up to 20 μm long, larger than most crystals observed in drill core. A sample from the north ramp portal (NRST-7-SSL, Table I) was analyzed for, but contained no detectable erionite, a fibrous zeolite carcinogenic to humans. The potential cancer risk associated with mordenite exposure at Yucca Mountain is indeterminate [9].

CALCITE AT EXILE HILL

Calcite is a common secondary mineral in the soil zone at Exile Hill and in subsurface fractures as well. Many Yucca Mountain studies utilize calcite to reconstruct the paleohydrology of the site. Recent investigations of fluid-inclusion gases in calcites have shown that the depositional environment can be identified from the content of H_2O, CH_4, N_2, Ar, and CO_2 trapped during precipitation [5,6]. Calcites formed under saturated conditions (e.g., hydrothermal veins and spring-deposited travertines) have H_2O-rich inclusions with a narrow range of N_2/Ar values, reflecting equilibrium with air, and either CO_2 or N_2 as the dominant inclusion gas. Pedogenic calcites have gas-rich (H_2O-poor) inclusions with high CH_4, and variable N_2/Ar ratios. The high CH_4 content is a by-product of anaerobic bacterial and fungal processes in the soil zone. Calcite inclusions from some locations have intermediate or variant compositions reflecting bulk analysis of inclusions trapped under alternating saturated and unsaturated conditions.

The Bow Ridge fault within 7 m of the surface at Exile Hill contains abundant calcite, but in the ESF 40 m below the surface, the fault is barren. Fluid inclusions in two samples of calcite closest to the fault in the ESF were analyzed. One is a laminated deposit from a small fault in pre-Rainier Mesa bedded tuffs 8 m west of the fault zone, and the other is coarse sparry calcite from a fracture with breccia in the Tiva Canyon Tuff 38 m east of the fault. Pedogenic calcite from a fracture within the Bow Ridge fault in densely welded Tiva Canyon Tuff near the surface of Exile Hill was analyzed for comparison with the ESF calcites.

Although the three samples are from the unsaturated zone, their fluid inclusions have water contents ≥99.2 mol % typical of saturated-zone calcites and much higher than the maximum of 86 % in pedogenic calcites from New Mexico [5,6]. In the drier climate of Yucca Mountain, calcite precipitation and recrystallization and carbonate transport may occur mostly when major meteoric recharge events create transient saturated conditions in the shallow subsurface. This may be especially true for pedogenic calcite within fractures in densely welded rock because the low-permeability fracture walls promote impoundment of water.

Fluid inclusions in the two ESF calcites are indistinguishable on the basis of CH_4, CO_2, N_2, and Ar proportions (Figure 1) despite the differences in crystal morphology and texture. The linear array of data in Figure 1A suggests the vein calcites contain an admixture of inclusions formed under unsaturated conditions and low CH_4-bearing inclusions typical of saturated conditions. A small but consistent difference between the very water-rich Tiva Canyon fracture filling and the more gaseous bedded tuff fault filling (Figure 1B) may be attributable to contrasting porosities of the fracture walls. When a fracture in very low-porosity densely welded tuff fills with water, local air is largely excluded. Water occupying a fracture in high-porosity nonwelded tuff is in contact with numerous rock pores that contain air, some of which is incorporated in the precipitating calcite.

POSSIBLE FUMAROLIC ALTERATION

A highly altered interval is located within pre-Pah Canyon tuffs just above the Topopah Spring Tuff in the Sta 10+25 to 10+45 interval. The intensely colored and disrupted tuffs have a dramatic impact that lends itself to questions about timing of hydrothermal processes. Clearly, a recently active hydrothermal system close to the potential repository would be a serious issue, albeit one that has already received close attention [7]. This study provides a beginning basis for comparison with other examples of hydrothermal alteration around Yucca Mountain.

The altered rock is a sequence of nonwelded bedded tuffs between the top of the Topopah Spring Tuff and the base of the Pah Canyon Tuff. The rocks are divided into five informal units A through E in chronological order (Figure 2). Mottled orange pink to reddish brown, medium- to coarse-grained pumiceous tuffs with some internal layering (unit A) predominate for several meters above the invert. Above this is a thinly laminated interval of fine-grained tuff up to ~2 m thick (unit B). This unit is overlain locally in former topographic depressions by a ~10-cm thick, fine-grained tuffaceous layer with disseminated coarser clasts (unit D). In one former ~30-cm depression developed on unit B, the lower 20 cm are filled by very fine-grained brown material (unit C) grading upward to unit D. Above unit D or directly overlying unit B is a sequence of mostly gray, fine-to coarse-grained nonwelded tuffs thinly bedded at the bottom (unit E).

The relative timing of alteration can be inferred from examination of depositional and erosional surfaces, evidence of soft and brittle deformation, fracturing, and faulting, and the distribution of secondary minerals. Most descriptions are based on the left rib exposure depicted in Figure 2.

Stratigraphic Contacts

The contact between units A and B, locally obscured by secondary alteration, is highly irregular with as much as several meters of relief. At some sites, such as around Sta. 10+26 and 10+38 to 10+40 (Figure 2), erosional relief on the unit A surface was covered by unit B material with relatively flat, undisturbed internal layering. In the Sta. 10+30 to 10+33 interval, some of the irregularities in the contact resulted from deformational interfingering of the two units.

Unit B consists of a lower part that has undergone both soft and brittle deformation mantled by an upper part with undeformed layering, well exposed in the 10+29 to 10+33 interval. The upper surface of the unit was very smooth as a result of surface scour. To the left of fault (b), the upper part of the unit was completely eroded.

Unit C occupies a single depression in the unit B surface around Sta. 10+29 to 10+30. This deposit could have been a mud pot or some other surficial expression of fumarolic activity. The fragments of unit B within this deposit do not appear any more altered than the unit B bedrock. The locally deposited unit D and the overlying unit E have simple flat contacts and little internal deformation. A soft-sediment slump is visible in unit E at Sta. 10+38 to 10+39.

Mineralogic Alteration

Alteration of the originally vitric tuffs was more intense in the rock exposed on the left rib than on the right rib but the general pattern of secondary mineral distribution is about the same. Unit A is altered to a smectite-rich assemblage with minor opal-CT and hematite (NR10+30SSL02,p1, NR10+32SSL01,p1 and p2, NR10+34SSL01,p2, Table I). Rock that was unaffected by the smectitic alteration was altered instead to heulandite-clinoptilolite with lesser amounts of smectite and opal-CT (NR10+34SSL01,p1, Table I). Heulandite-clinoptilolite with subequal amounts of Ca and K as the exchangeable cations and smaller amounts of light-colored smectite are common fracture coatings where the smectitic altered tuffs are brecciated. A bleached alteration front is visible within Unit A on the left rib at Sta. 10+35 to 10+43. The width of the bleached zone is highly irregular and may be as much as one meter or more. In some places the front moved preferentially through certain layers in the tuff, but elsewhere the front transgressed layering.

Prominent silicification in unit B resulted in replacement of the tuff by opal-CT (NR10+30SSL01,p2, Table I), producing a chalky to porcellaneous rock with grayish orange to pale grayish orange pink, pale yellowish brown, and white colors. Rock that escaped silicification was subsequently altered to a smectite-clinoptilolite assemblage (NR10+30SSL01,p1, Table I).

Distinctive nodules on the left rib within broken blocks of lower unit B are pale yellowish brown to grayish blue microcrystalline quartz, cristobalite, and opal-CT with fractures containing drusy quartz crystals (NR10+33SSL01,p1,p2, Table I). Scattered fluorite crystals and a few fluorite-filled fractures are present.

Mineralogic analysis of units C and D awaits further sampling. Unit E has been zeolitized to an assemblage dominated by heulandite-clinoptilolite (NR10+32SSL02,p1 and p2, Table I). A few fractures with apertures less than 1 mm contain microcrystalline quartz and botryoidal spheres of opal-CT at the margins. Heulandite-clinoptilolite encrusts the spheres, suggesting that zeolitization postdated the fracture fillings.

Faulting, Fracturing, and Alteration

Of the four main faults and fractures exposed on the left rib, only the diagonal fault/fracture labeled (a) in Figure 2 is associated with deformation and alteration in units A and B. The fracture is parallel to bedding in the lower part of unit A, but higher up it follows the boundary of a rotated block and a discontinuity in bedding. Unit B is highly disrupted in a 2-m-wide zone centered on the fracture, but few discontinuities coincide with the fracture trace. Units C, D, and E are offset less than 1 cm along the fracture. The observed deformation could be attributed to early episodes of brecciation, faulting, and alteration affecting units A and B, followed by deposition of units C, D, and E and propagation of a fracture upward into the younger units during a minor late adjustment. Early faulting at this location could help explain the surface depression formed on unit B and filled by units C and D. The apparent absence of offset at the A-B contact may be explained by lateral displacement of the brecciated rocks.

Fault (b) has ~1 m of displacement. If the walls of the fault are conceptually positioned to reunite the unit E contact, the quartz-cristobalite nodules in unit B on the left wall match up with the alteration front on the right wall. Faults (c) and (d) both offset the alteration front in unit A and, like fault (b), postdate the alteration that produced the bleached zones.

DISCUSSION AND SUMMARY

The first 1.1 km of the ESF contains evidence of fluid-rock interaction under a variety of conditions. Vapor-phase mineral deposition, brecciation, and breccia cementation in the Tiva Canyon Tuff occurred as the pyroclastic deposit cooled. Calcite in faults and fractures was deposited under conditions of transient local water saturation within the unsaturated zone.

Alteration in the two lower units A and B of the pre-Pah Canyon tuffs shows mineralogic affinities – the presence of quartz, cristobalite, and fluorite – with syngenetic devitrification and vapor-phase alteration products in the underlying Topopah Spring Tuff. Silicified tuffs with cristobalite at the top of the Topopah Spring Tuff also exist in isolated outcrops of southern Yucca Mountain and Busted Butte east of the mountain [10]. Smectite was not observed at the outcrop sites, perhaps due to preferential weathering, but smectitic alteration at the top of the Topopah Spring Tuff has been noted in drill core [11]. Brecciation at the ESF site is another feature in common with the alteration in outcrop. The smectitic alteration seems to have been more localized than the later zeolitization. The localization of the smectitic alteration argues against a pedogenic origin even though units A and B were subaerially exposed and may have undergone pedogenic modification.

Zeolitization of the pre-Pah Canyon tuffs was a separate alteration event. The upper units D and E had not yet been deposited when units A and B were undergoing brecciation, smectitic alteration, silicification, and erosion. Zeolitic alteration of nonwelded tuffs at or just above the

top of the Topopah Spring Tuff has been noted in drill core and outcrop at northeastern Yucca Mountain [12,13]. The hydrologic, geochemical, and perhaps thermal conditions that favored zeolitization of only certain areas in this stratigraphic interval have yet to be determined.

ACKNOWLEDGMENTS

This study benefited substantially from discussions with members of the U.S. Bureau of Reclamation, especially Steve Beason. Reviews by J. W. Carey and two anonymous reviewers are greatly appreciated. This work was supported and managed by the U.S. Department of Energy, Yucca Mountain Site Characterization Office. D. Norman's research was supported by the Waste-Management Education and Research Consortium. The record package containing traceability information is LA-EES-1-TIP-95-021.

REFERENCES

1. Sandia National Laboratories, "Administrative Ramp Cross Section: Lithology and Borehole Projections," Drawing No. 88-60-09, Version QA1.7 (1994).

2. F. Chung, Journal of Applied Crystallography **7**, p. 519 (1974).

3. S. Chipera and D. Bish, Los Alamos National Laboratory report LA-11663-MS (1989).

4. D. Bish and S. Chipera, Clays and Clay Minerals **39**, p. 437 (1991).

5. M. Gundimeda, "Environmental Gas Analysis of Fluid Inclusions in Calcium Carbonates from New Mexico, Including Vein Calcites from Los Alamos National Laboratory, Using Quadrupole Mass Spectrometry," MS Thesis, New Mexico Tech., Socorro, NM, 141 pp. (1995).

6. B. Newman, D. Norman, M. Gundimeda, and S. Levy, Chem. Geology (in press).

7. National Research Council, Ground Water at Yucca Mountain: How High Can It Rise? National Academy Press, Washington, D. C., 231 pp. (1992).

8. D. Cowan, V. Priest, and S. Levy, Appl. Radiat. Isot. **44**, p. 1035 (1993).

9. G. Guthrie Jr., D. Bish, S. Chipera, and R. Raymond, Jr, Los Alamos National Laboratory report LA-12573-MS (1995).

10. S. Levy, in Scientific Basis for Nuclear Waste Management XVI, edited by C. Interrante and R. Pabalan (Mater. Res. Soc. Symp. Proc. 294, Pittsburgh, PA 1993), p. 543-548.

11. W. Carr, U.S. Geol. Survey Open-File Report 82-457 (1982).

12. D. Broxton, D. Vaniman, F. Caporuscio, B. Arney, and G. Heiken, Los Alamos National Laboratory report LA-9324-MS (1982).

13. D. Broxton, S. Chipera, F. Byers, Jr., and C. Rautman, Los Alamos National Laboratory report LA-12542-MS (1993).

TABLE I

Quantitative X-Ray Diffraction Results for ESF North Ramp (wt. %)

Sample	Smectite	Clino-ptilolite	Mord-enite	Cristo-balite	Opal-CT	Feldspar	Quartz	Hematite	Fluorite	Erionite	Total
NRST-7-SSL[1] SPC 501015	4±2[2]	2±1	57±27	3±2	n.d.[3]	26±16	8±3	n.d.	n.d.	b.d.l.[4]	100±27
NR10+30SSL01,p1 SPC 509174	16±5	7±1	n.d.	n.d.	67±18	14±2	5±1	n.d.	n.d.	n.a.	109±19
NR10+30SSL01,p2 SPC 509174	3±1	1±1	n.d.	n.d.	109±22	n.d.	5±1	n.d.	n.d.	n.a.	118±22
NR10+30SSL02,p1 SPC 509175	91±27	5±1	n.d.	n.d.	5±1	8±1	trace[5]	n.d.	n.d.	n.a.	109±27
NR10+32SSL01,p1 SPC 510522	95±29	4±1	n.d.	n.d.	11±2	2±1	trace	1±1	n.d.	n.a.	113±29
NR10+32SSL01,p2 SPC 510522	99±30	1±1	n.d.	n.d.	1±1	4±1	trace	1±1	n.d.	n.a.	106±30
NR10+32SSL02,p1 SPC 509187	5±2	73±5	n.d.	n.d.	10±3	12±3	3±1	n.d.	n.d.	n.a.	103±7
NR10+32SSL02,p2 SPC 509187	6±2	59±5	n.d.	n.d.	25±7	12±2	4±1	n.d.	n.d.	n.a.	106±9
NR10+33SSL01,p1 SPC 509117	trace	n.d.	n.d.	n.d.	n.d.	n.d.	95±5	n.d.	trace	n.a.	95±5
NR10+33SSL01,p2 SPC 509117	n.d.	n.d.	n.d.	40±5[6]	10±5[6]	n.d.	49±2	n.d.	1±1	n.a.	100±5
NR10+34SSL01,p1 SPC 510523	15±5	70±5	n.d.	n.d.	10±2	5±1	1±1	n.d.	n.d.	n.a.	101±7
NR10+34SSL01,p2 SPC 510523	74±22	19±1	n.d.	n.d.	1±1	6±1	trace	trace	n.d.	n.a.	100±22

[1]Results for this sample are semi-quantitative due to small sample size.
[2]Errors are conservative 2-sigma values.
[3]n.d. = not detected.
[4]For erionite only, b.d.l. means below the detection limit (~ 100 to 500 ppm) utilizing specialized analytical techniques. For samples not analyzed using the special methods, undetected erionite is reported as n.a. = not analyzed.
[5]trace = less than 0.5 weight percent.
[6]Proportions of cristobalite and opal-CT are approximate.

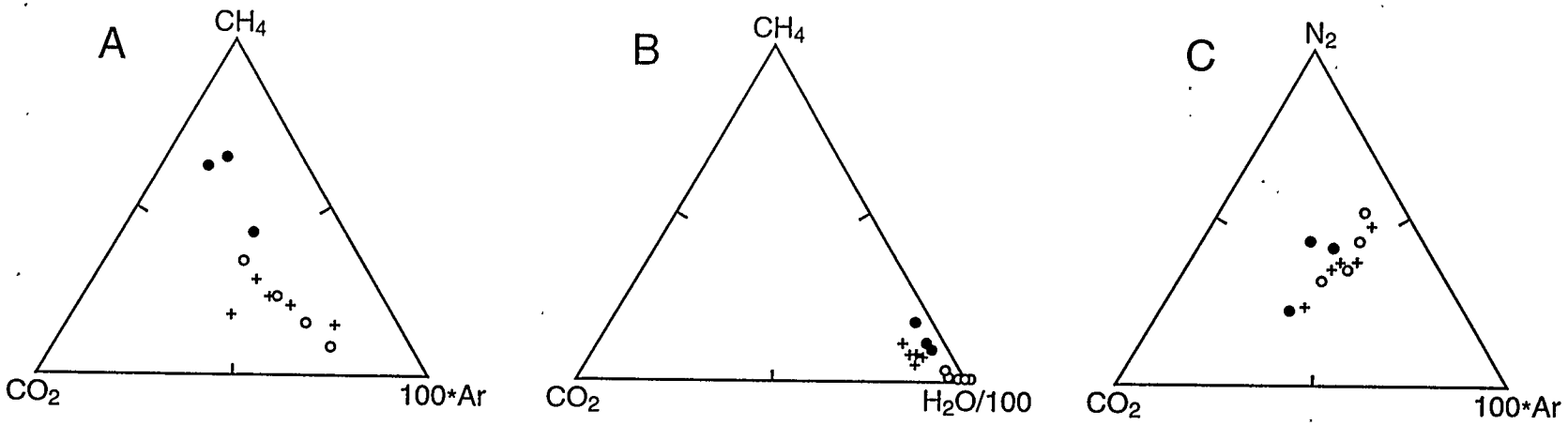

Figure 1. Ternary diagrams showing molecular proportions of water and gases in calcite fluid inclusions. Sample symbols are (•) TR14-10-SSL pedogenic calcite; (+) NR-1-SSL laminated fault filling in nonwelded tuff; (o) NR-2-SSL sparry fracture filling in densely welded tuff.

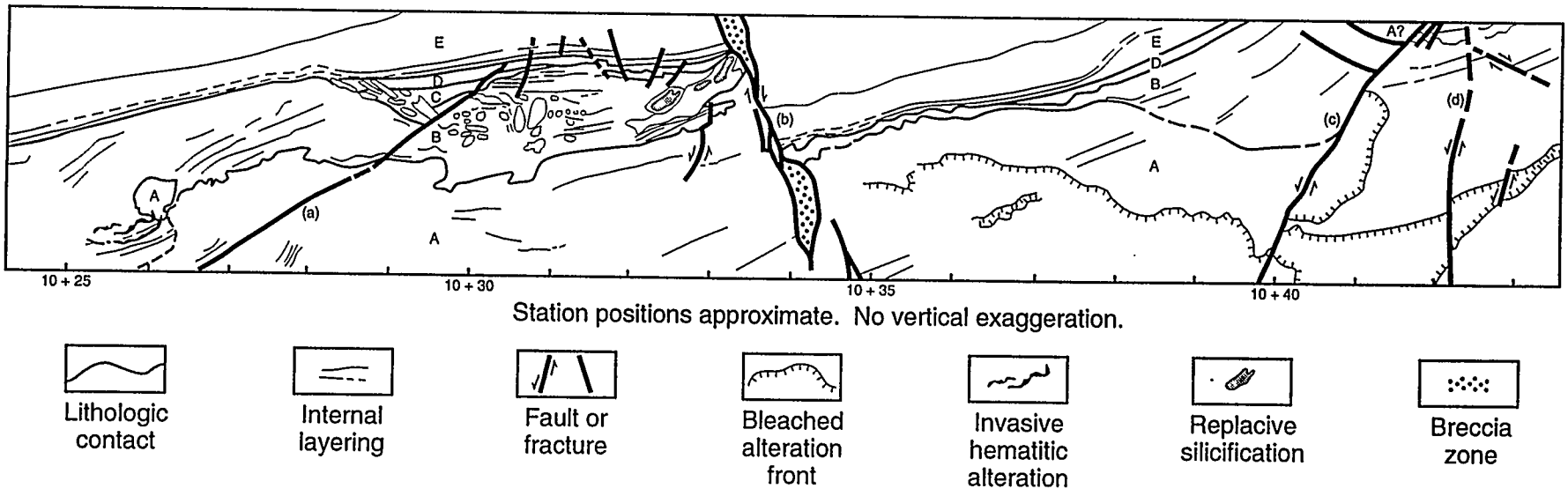

Figure 2. Wall map of possible fossil fumarole, ESF north ramp, left rib.

DISCLAIMER